A near-infrared phosphorescent iridium(III) complex for fast and time-resolved detection of cysteine and homocysteine

Yuanyan Li,[a,b] Yongquan Wu,[b] Jie Wu,[b] Weican Lun,[b] Hong Zeng[b] and Xiaolin Fan*[a,b]

[a] College of Chemistry, Nanchang University, 999 Xuefu Avenue, Nanchang 330031, P. R. China, E-mail: fanxl@gnnu.edu.cn

[b] School of Chemistry and Chemical Engineering, Gannan Normal University, Ganzhou 341000, P. R. China

Experimental section

Materials

All reagents were purchased from commercial suppliers and used without further purification. Unless specified, they were purchased from Shanghai Titan Scientific Co., Ltd (China). 2-benzothienylboronic acid was purchased from Shanghai Sain Chemical Co., Ltd (China). Tetrakis (triphenylphosphine) palladium (0) ($Pd(PPh_3)_4$) and $IrCl_3 \cdot 3H_2O$ were purchased from Shanxi Rock New Material Co., Ltd (China). Acetophenone and 2,2'-bipyridine-4,4'-dicarbaldehyde were purchased from Zhengzhou Alfa Chemical Co., Ltd (China). K_2CO_3, Na_2SO_4 and NaOH were purchased from Tianjin Damao Chemical Reagent Factory (China). Methyl thiazolyl tetrazolium (MTT) and fetal bovine serum (PBS) were purchased from Jiangshu Beyotime Biotechnology Co., Ltd (China). RPMI 1640 nutrient solution was purchased from Lanzhou Bailing Biotechnology Co., Ltd (China). 1-chloroisoquinoline, alanine (Ala), arginine (Arg), aspartic acid (Asp), asparagine (Asn), cysteine (Cys), homocysteine (Hcy), glutamic acid (Glu), glutamine (Gln), glycine (Gly), histidine (His), isoleucine (Ile), leucine (Leu), lysine (Lys), methionine (Met), phenylalanine (Phe), Proline (Pro), threonine (Thr), tryptophan (Trp), tyrosine (Tyr), valine (Val), Serine (Ser), glutathione (GSH), were purchased from Aladdin Technology Co., Ltd (China). Agarose (low gelling temperature) was purchased from Shanghai Macklin Biochemical Co., Ltd (China).

Instruments

^1H NMR spectra were obtained on a Bruker DRX-400 NMR spectrometer

(Germany) with tetramethylsilane (TMS) as internal standard. High resolution mass spectra (HRMS) were obtained with an ESI ionization sources on a Bruker Maxis 4G (Data analysis 4.0) instrument (Germany). UV-Vis absorption spectra were recorded on a Shimadzu UV-2700 spectrophotometer (Japan). Emission spectra were recorded on an Edinburgh FS5 fluorescence spectrophotometer (UK). Time-resolved emission spectra were measured on a PTI Quanta Master Fluorescence System (Photo Technology International). Cell imaging experiments were performed on an Olympus FV1000 laser scanning confocal microscopy (Japan). Zebrafish imaging experiments were performed on a Leica TCS-SP8 laser scanning confocal microscopy (Germany). The absorbance values in MTT assay were measured using a Varioskan LUX microplate reader (Thermo Fisher Scientific Inc, USA). Mouse imaging experiments were carried out using an IVScpoe 7550 *in vivo* imaging system (Shanghai CLINX, China).

UV–Vis absorption and emission spectra

Absorption and emission spectra were detected with 1.0 cm quartz colorimetric dishes at room temperature. The luminescence intensity was measured at $\lambda_{ex/em}$ = 500/683 nm. The concentration of FNO1 was 10 μM in DMSO/PBS buffer solution (pH = 7.4, v/v 1:4).

The luminescence quantum yields were measured using tris-(2,2'-bipyridyl)-ruthenium(II) chloride hexahydrate (Φ = 0.063 in DMF) as a standard and were calculated according to equation: $\Phi_\mu = \Phi_s I_\mu A_s N_\mu^2 / I_s A_\mu N_s^2$, where, 'N' is the refractive index of the solvent, 'I' is the integrated area of emission intensity, 'A' is the absorbance at the excitation wavelength, and the subscripts 'μ' and 's' refer to the reference sample and the sample, respectively.[1]

Computational details

These iridium complexes were optimized with density functional theory (DFT) using the PBE functional (B3LYP),[2,3] a functional that has been widely employed in previous studies of iridium complexes.[4] The "double-ζ" quality basis set LANL2DZ

and corresponding effective core potentials were used for iridium atom, while the 6-31G (p, d) basis set was used on nonmetal atoms in the gradient optimizations.[5] Calculations were performed with Gaussian 09 (Revision D.01).[6] To shed more light on the nature of the excited states of these Ir(III) compounds, vertical transition energies were calculated on the basis of the optimized S0 and T1 structures via time-dependent DFT (TD-DFT).[7]

Cell culture and cytotoxicity assay

Cytotoxicity was measured by performing MTT colorimetry on MCF-7 cells provided by the Institute of Biochemistry and Cell Biology (Chinese Academy of Sciences). Logarithmic growth phase of MCF-7 cells in RPMI 1640 nutrient solution were seeded into a transparent 96-well flat-bottomed microplate (about 5×10^4 cells/well, 100 μL/well), then cultured at 37 ^oC, under 5% CO_2 atmosphere for 24 h.

When the former nutrient solution was removed, fresh nutrient solution (100 μL/well) and different concentrations of FNO1 solution (0, 5, 10, 15, and 20 μmol/L, diluted in RPMI 1640 nutrient solution, 100 μL/well) were added.

24 h after, 100 μL nutrient solution and 20 μL MTT solution (5 mg/mL) was added to each well after the former solution was removed, and the cells continued to be incubated for 5 h at the same conditions. The former mixed solution was discarded and 150 μL DMSO was added into every well. Oscillate microplate for 10 minutes to ensure that the formazon crystals were fully dissolved. The absorbance value of each well at 570 nm was measured by microplate reader. Cell viability (%) = (mean of Abs. value of treatment group/mean of absorbance value of control group) × 100%.

Table S1 Photophysical data of FNO1, FNO1+Cys, and FNO1+Hcy

Sample	$\lambda_{abs,peak}$/nm (ε/dm^3 mol^{-1} cm^{-1})	$\lambda_{FI,peak}$/nm	Φ_{em}	Detection limit/μM
FNO1	486 (4400), 303 (25600)	683, 748	0.005	
FNO1+Cys	486 (5700), 358 (13400), 310 (23000), 286 (22300)	683, 748	0.109	0.228
FNO1+Hcy	486 (6200), 358 (14200), 311 (23200), 285 (22800)	683, 748	0.122	0.134

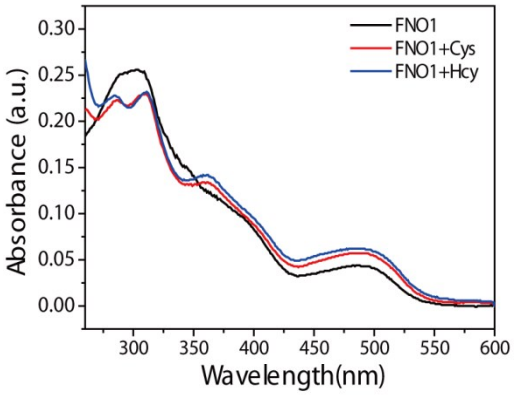

Fig. S1 UV-Vis absorption spectra of FNO1 (10 μM), FNO1 (10 μM) + Hcy (140 μM), FNO1 (10 μM) + Cys (140 μM).

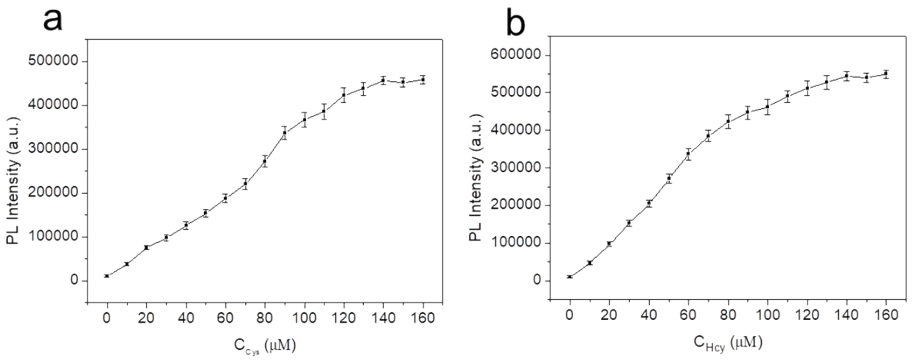

Fig. S2 Luminescence intensity of FNO1 (10 μM) + Cys/Hcy at 683 nm with the change of (a) Cys and (b) Hcy concentration, λ_{ex} = 500 nm, λ_{em} = 683 nm.

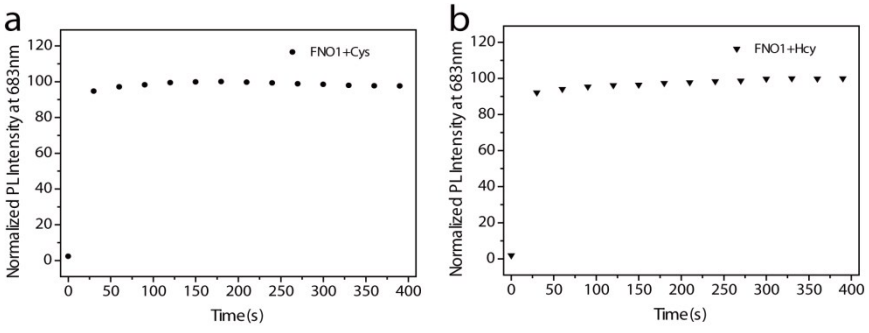

Fig. S3 Changes of luminescence intensities of (a) FNO1 (10 μM) + Cys (140 μM) and (b) FNO1 (10 μM) + Hcy (140 μM) with different time.

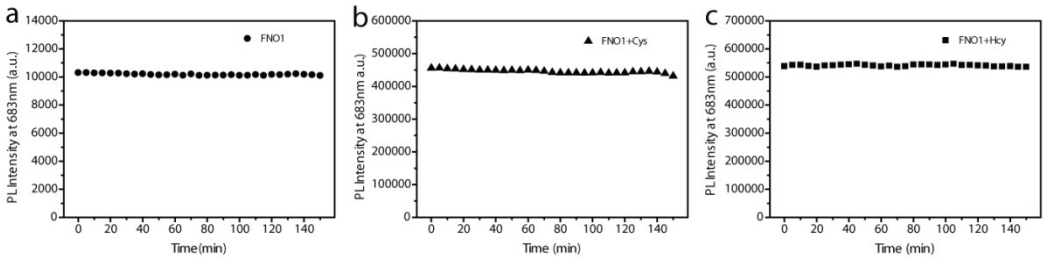

Fig. S4 Changes of luminescence intensities of (a) FNO1, (b) FNO1+Cys, and (c) FNO1+Hcy irradiated at 500 nm for 2.5 h.

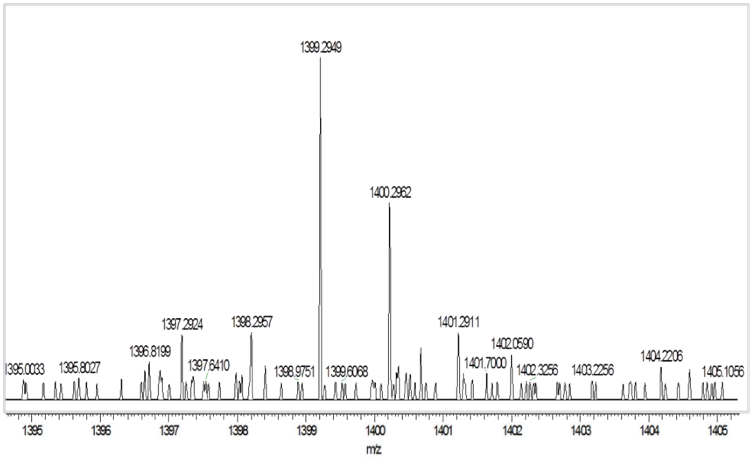

Fig. S5 HR-MS of FNO1+Hcy.

Table S2. Frontier molecular orbital energies (in eV) calculated at the B3LYP/[LANL2DZ-ECP/6-31G*] level

Sample	HOMO-2	HOMO-1	HOMO	LUMO	LUMO+1	LUMO+2	GAP
FNO1	-8.04	-7.44	-7.37	-5.22	-4.88	-4.47	2.15
FNO1+Cys	-7.69	-7.03	-6.95	-4.22	-3.81	-3.79	2.74
FNO1+Hcy	-7.79	-7.13	-7.09	-4.44	-3.95	-3.90	2.64

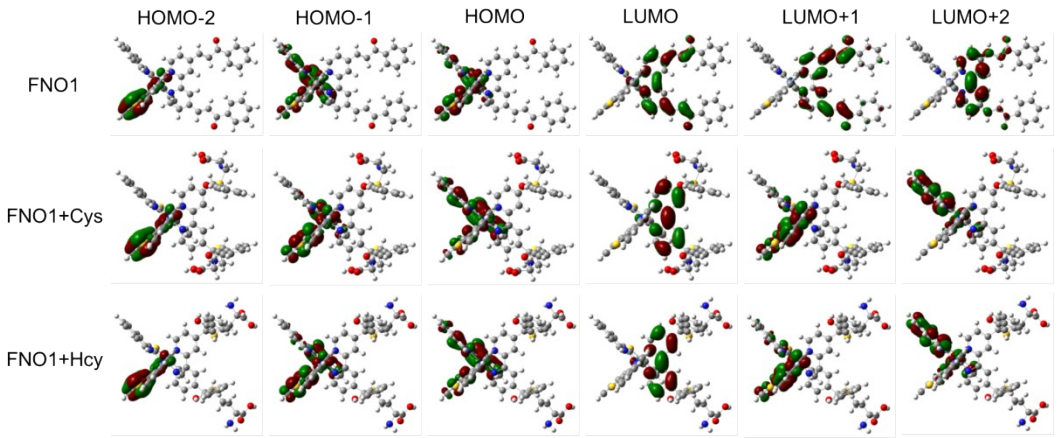

Fig. S6 Representations of the frontier molecular orbitals (MOs) for the S_0 geometry of complex FNO1, FNO1+Cys, and FNO1+Hcy as determined at the B3LYP/[LANL2DZ-ECP/6-31G*] level.

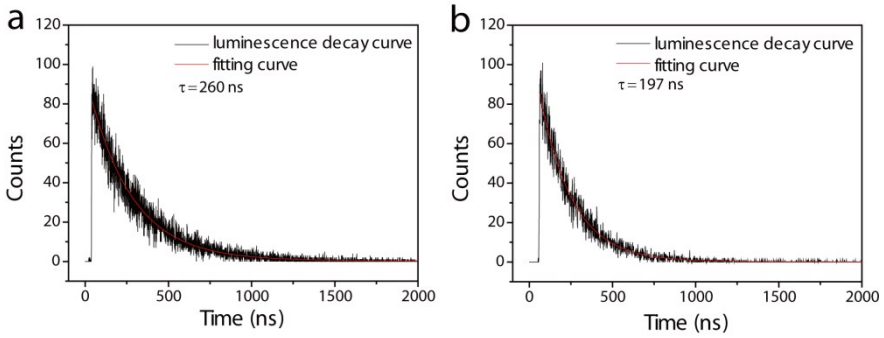

Fig. S7 Decay curve, fitting curve and fitted luminescence lifetime of (a) FNO1+Cys and (b) FNO1+Hcy, 10 μM in CH_3OH, $\lambda_{ex/em}$ = 500/683 nm

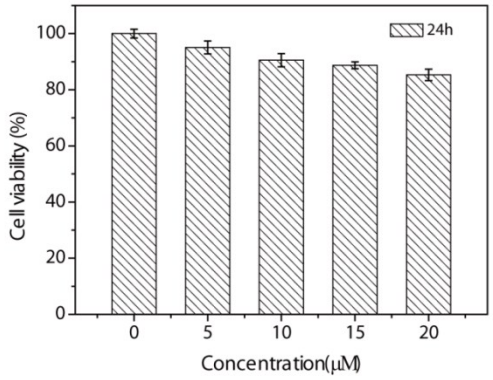

Fig. S8 Cell viability values (%) detected by MTT method versus different incubation concentrations (0–20 μM) of FNO1.

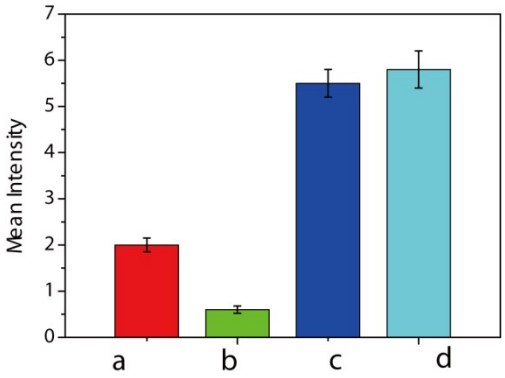

Fig. S9 Quantification of mean luminescence intensity in Fig. 6 a–d. Emission was collected by a NIR channel at 650−750 nm under excitation with 515 nm laser.

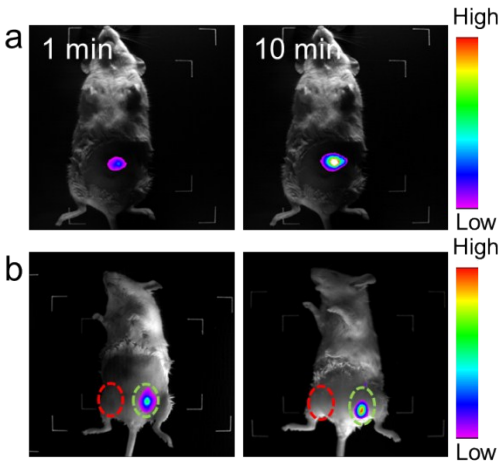

Fig. S10 NIR luminescence images of shaved living mice. (a) mouse was subcutaneously injected in abdomen with Hcy (40 μM, 100 μL) and FNO1 (10 μM, 100 μL), the images were captured after 1 min and 10 min. (b) mice injected with 100 μL normal saline + 100 μL FNO1 (left groin), Hcy (100 μL) + 100 μL FNO1 (right groin), the concentrations of Hcy were 80 μM (left mouse) and 150 μM (right mouse), the images were captured after 10 min. Emissions were collected at > 650 nm as detection signals, upon irradiation at 532 nm laser.

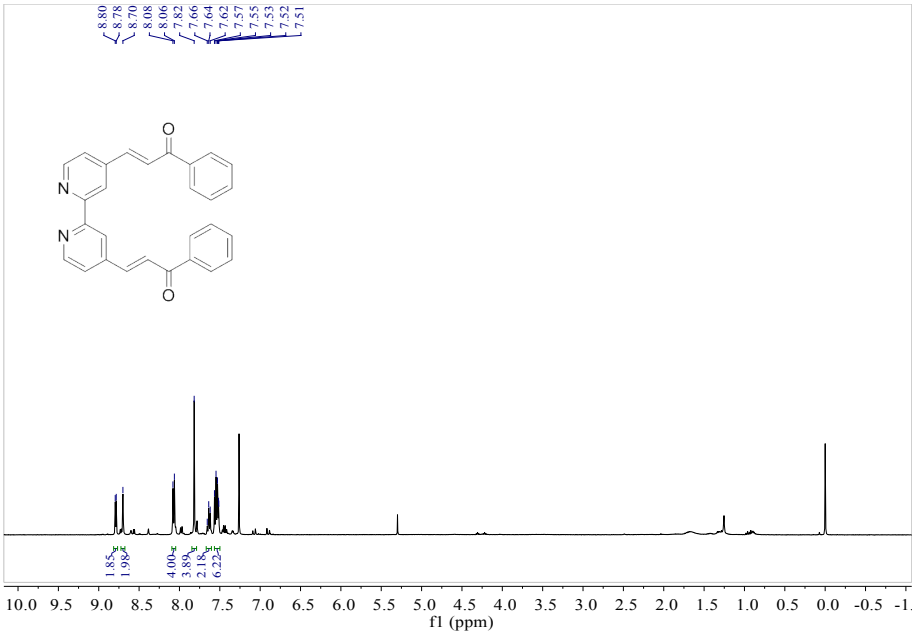

Fig. S11 ^{1}H NMR (400 MHz, $CDCl_3$) spectrum of L1

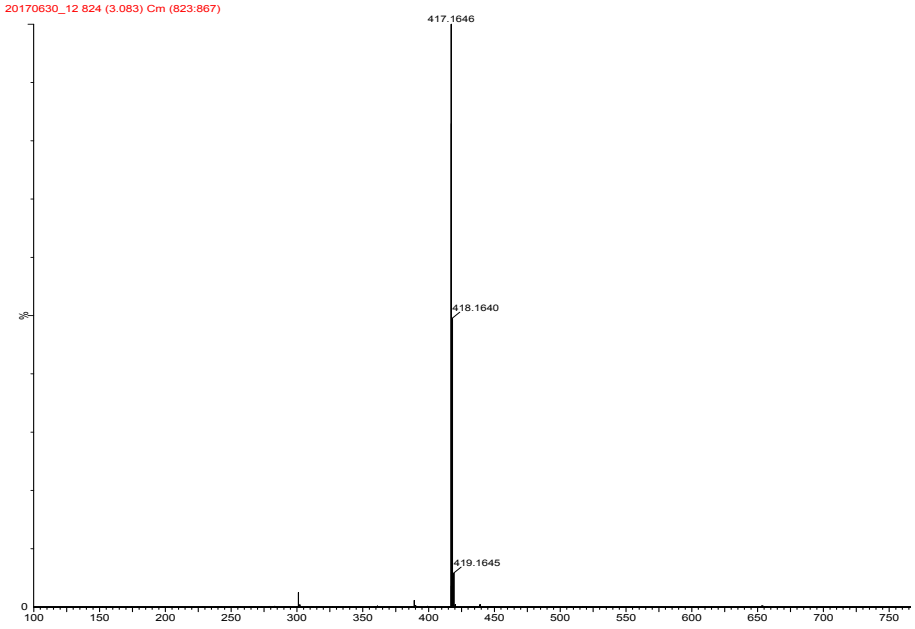

Fig. S12 HR-MS of L1

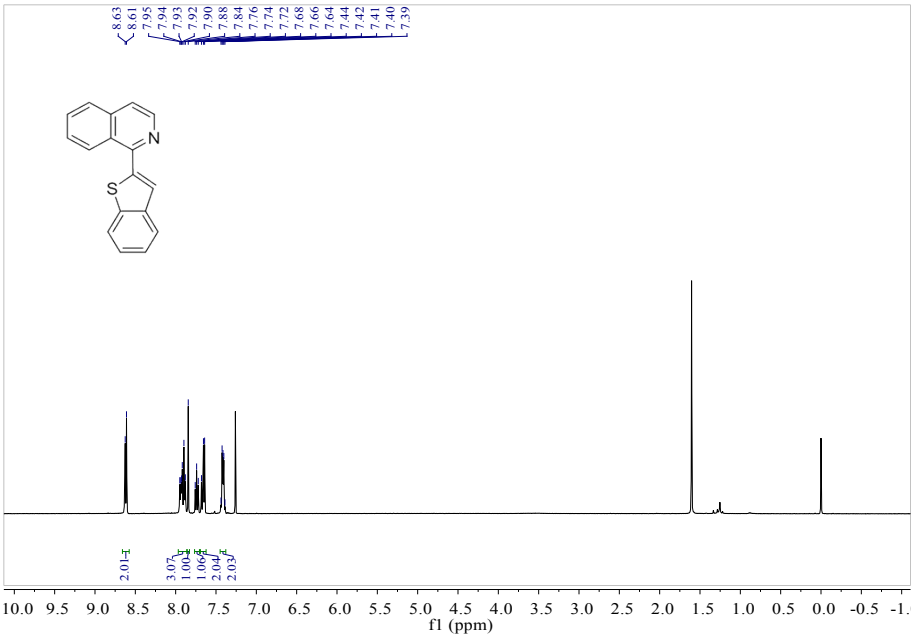

Fig. S13 ^{1}H NMR (400 MHz, $CDCl_3$) spectrum of L2

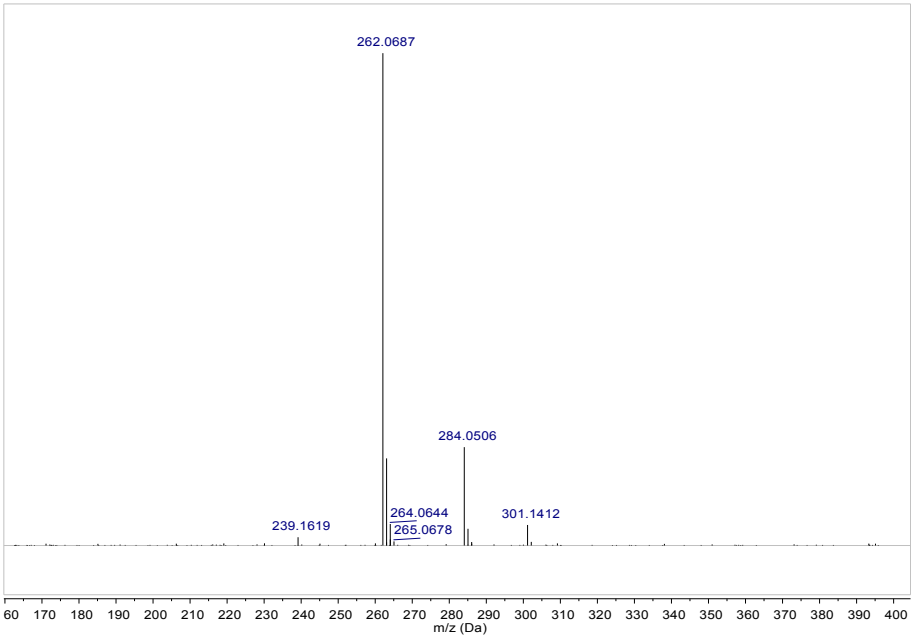

Fig. S14 HR-MS of L2

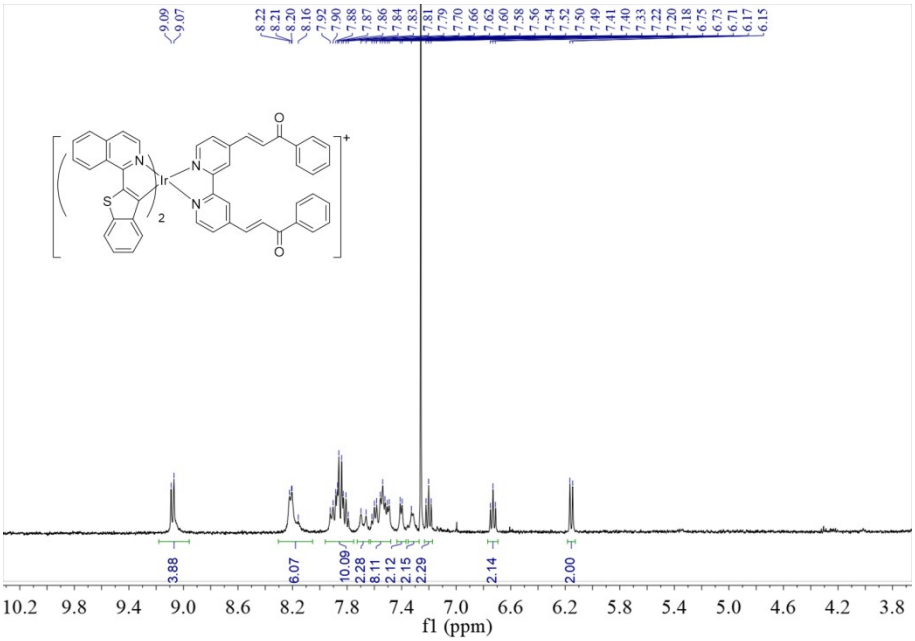

Fig. S15 ^{1}H NMR (400 MHz, $CDCl_3$) spectrum of FNO1

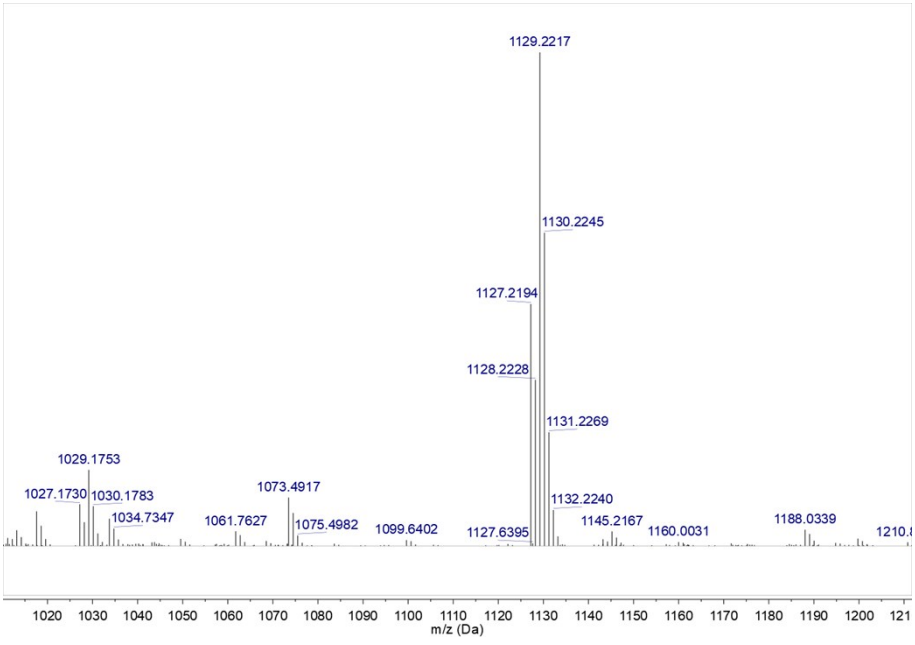

Fig. S16 HR-MS of FNO1

1. J. M. Elbicki, D. M. Morgan and S. G. Weber, *Anal. Chem.,* 1985**, 57**, 1746.

2. (a) G. A. Crosby and J. N. Demas, *J. Phys. Chem.*, 1971, **75**, 991. (b) J. V. Caspar and T. J. Meyer, *J. Am. Chem. Soc.,* 1983, **105,** 5583.

3. C. Adamo and V. Barone, *J. Chem., Phys.*, 1999,**110**,6158.

4. (a) H. F. Li, P. Winget, C. Risko, J. S. Sears and J. L. Brédas, *Phys. Chem. Chem.*

Phys., 2013, **15**, 6293. (b) J. Y. Hung, C. H. Lin, Y. Chi, M. W. Chung, Y. J. Chen, G. H. Lee, P. T. Chou, C. C. Chen and C. C. Wu, *J. Mater. Chem*., 2010, **20**, 7682. (c) X. N. Li, Z. J. Wu, Z. J. Si, H. J. Zhang, L. Zhou and X. J. Liu, *Inorg. Chem*., 2009, **48**, 7740.

5. (a) P. J. Hay and W. R. Wadt, *J. Chem. Phys*., 1985, **82**, 270. (b) W. R. Wadt and P. J. Hay, J. Chem. Phys., 1985, **82**, 284. (c) P. J. Hay and W. R. Wadt, *J. Chem. Phys*., 1985, **82**, 299.

6. M. J. Frisch, G. W. Trucks, H. B. Schlegel, G. E. Scuseria, M. A. Robb, J. R. Cheeseman, G. Scalmani, V. Barone, B. Mennucci and G. A. Petersson, *et al*. Gaussian 09, Revision D.01; Gaussian, Inc.: Wallingford, CT, 2009.

7. S. Fantacci, F. D. Angelis and A. Selloni, J. Am. Chem. Soc. 2003, **125**, 438.